Advances in Aerodynamics

RESEARCH Open Access

Enhancement of scramjet inlet efficiency by geometrical modifications

Dinesh Kumar Bajaj[1*], Sakshi Tushar Kansara[1], Nayani Kishore Nath[2], Ashish Vashishtha[3] and Devabrata Sahoo[4]

[1] Department of Aerospace Engineering, School of Engineering and Sciences, MIT Art, Design and Technology University, Pune 412201, India
[2] Advanced Systems Laboratory, Defence Research and Development Organization, Hyderabad 500058, India
[3] Department of Aerospace and Mechanical Engineering, South East Technological University, Carlow R93 V960, Ireland
[4] Department of Aerospace Engineering, Graphic Era (Deemed to Be University), Dehradun 248002, India

Abstract

Scramjets are considered one of the important propulsion systems for realizing hypersonic flights and have attracted a lot of research interest over the past few decades. The present study focuses on conducting a comprehensive numerical investigation on a scramjet inlet-isolator at Mach 5 with the motivation to improve efficiency. The study investigates a two-dimensional scramjet inlet-isolator, analyzing both external and internal flow characteristics by using the commercially available tool Ansys-Fluent. Numerical simulation is the first step to incorporate the passive bleed mechanism into the inlet design features with alterations aimed at improving airflow regulation. The subsequent investigation is the analysis of the effect of a number of cowl deflection angles on performance of the positions. An extensive evaluation is presented on the effect of varying cowl deflection angles on the inlet isolator efficiency. A combined approach is also adopted in the study whereby the most promising configurations from the bleed mechanism and cowl deflection angle studies are incorporated into a single geometry. This aims at increasing the inlet isolator efficiency and the pressure recovery. The aim of this integrated strategy is to develop an inlet geometry that is optimal for performance of the engine and pressure recovery capability enhancement. The study analyzes ten different cases, and it is noted that out of these, the 4-degree cowl deflection angle is the most efficient in enhancing the total pressure efficiency.

Keywords: Scramjets, Inlet-isolator, Flow control techniques, Passive boundary layer bleed, Lip-shock-induced separation, Total pressure recovery

1 Introduction

The scramjet engine is a new type of propulsion system that offers many advantages for aircraft operating at high speeds. This type of engine is particularly suitable for hypersonic flight due to its ability to maintain speed in the hypersonic range. Air can be maintained at supersonic speeds thanks to technological advances in the piezoelectric inlet and the scramjet engine's pressure-generating combustors. Combustor ensures air, fuel, and air swirl to enhance the combustion process before being directed to the nozzle, where the mixing is easily achieved for effective thrust generation. It continues to play a key role in maintaining the hypersonic velocity by utilizing advanced air/fuel

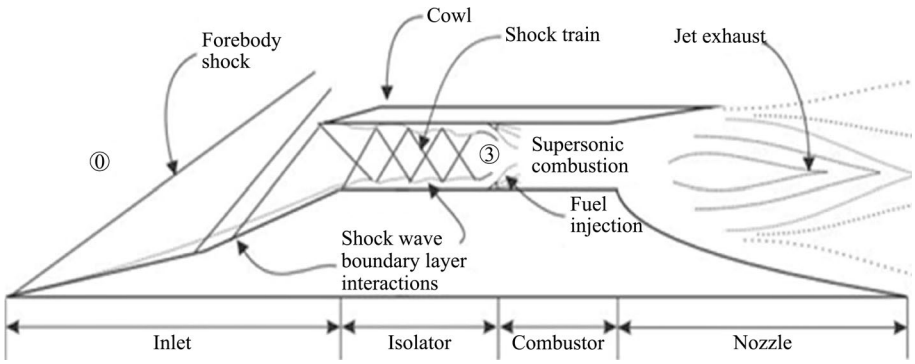

Fig. 1 A general diagram illustrating the layout of a scramjet engine and elucidating its operational concept [1]

combustion methods. The stability of advanced scramjet engines relies on the inlet; therefore, it is important to understand the advanced engine's inlets and their functions.

With the air entering the inlet at hypersonic velocities, it first slows down and compresses; and next, it moves into the combustion chamber to which fuel is pumped and combustion occurs at supersonic speeds. It then passes through the nozzle and thrust is generated. A detailed explanation of the flow characteristics and shock processes within the inlet is important for enhancing engine performance. The crucial parts and operation of the scramjet engine are presented in Fig. 1.

Several important aspects of inlet flow phenomena need to be taken into account, such as boundary layer transition, shock wave-boundary layer interactions (SWBLI), boundary layer separation, glancing shock interactions, and other significant aspects. The effectiveness and efficiency of propulsion systems can only be increased by comprehending and managing these basic inlet flow phenomena, which puts them at the center of ongoing research and development initiatives.

2 Literature review and objective

This paper presents a comprehensive review in the field of scramjet engine, covering important and critical factors such as design, analysis, and experimental results. Che Idris et al. [1] conducted experiments using pressure-sensitive paint as a non-intrusive technique to study scramjet inlet fluid mechanics at Mach 5 with the objective of extracting information about flow characteristics and improving performance evaluation capability. Im and Do [2] with regard to scramjets stated that for safe flights it is essential to understand flow choking-induced unstart, which includes knowledge of the choking mechanism diagnostic indicators and control in both open and closed loops. Rodi et al. [3] analyzed time-accurate pressure measurements in a dual-mode ramjet/scramjet inlet, finding that increasing inlet back-pressure enhances pressure signal variability, inlet contraction ratio significantly impacts pressure measurements, unstart manifests as a high-pressure wave moving upstream, and cowl-induced unstart triggers oscillatory behavior centered around 300 Hz. Smart [4] emphasized the pivotal role of scramjet inlets in hypersonic engines, with their design profoundly influencing engine performance. He advocates setting compression levels based on combustor pressure and emphasize the potential of three-dimensional inlet

configurations for efficient operation at Mach 6 to 12. Smart [5] found that optimal two-dimensional scramjet inlets for maximum total pressure recovery have shocks with nearly equal strength, even with additional constraints imposed by scramjet requirements, and that the method of Lagrange multipliers is efficient for optimization in this context. Ogawa and Boyce [6] conducted multi-objective design optimization for axisymmetric scramjet inlets, revealing the influence of parameters like inlet exit radius and highlighting the advantages of Busemann-type geometries for high-performance designs. Suresh et al. [7] conducted numerical optimization studies to maximize total pressure recovery and minimize shock interactions in a supersonic inlet design, validating the proposed methods against theoretical data and CFD simulations. Neale and Lamb [8] observed that a two-dimensional combined external/internal compression intake achieved a maximum pressure recovery of 87% at a Mach number of 2.2, with potential for further improvement to 90%, highlighting the importance of bleed slot design and efficient subsonic diffusion rates. Häberle and Gülhan [9] examined a scramjet inlet at Mach 7, finding that a passive bleed reduces separation bubbles but requires precise placement. Increasing internal contraction ratios doesn't cause unstart, suggesting sidewall compression for multi-engine setups. The inlet is self-starting and manageable despite being more complex in design with no unforeseen effects reported. For example, Häberle and Gülhan [10] performed an experimental study on a fixed geometry scramjet inlet operating at Mach 6, aiming to examine the influence of viscous effects, boundary-layer bleed integration, and varying backpressure on the internal flow field and heat transfer. Additionally, passive bleed effects in controling separation bubbles and measuring heat transfer coefficients using infrared thermography were also tested. Passive boundary layer bleed was shown to be effective, while Häberle and Gülhan [11] performed an experimental investigation at Mach 7, illustrating the efficient functioning of a passive boundary layer bleed, maintaining safe levels of inlet start risk, and offering quality infrequent data for SCRAM-jet propulsion development, and CFD validation. Focus on the design of a Mach 7 to Mach 8 scramjet nozzle for the DFG project was continued in the work of Häberle and Gülhan [12], who also identified the importance of passive boundary layer bleed as a specific feature of a fixed geometry scramjet inlet to reduce un-start risk in mud-sponsored studies modeling a Mach 6 flow. In their experimental study at Mach 7, Häberle and Gülhan [13] examined the viscous effects of a two-dimensional scramjet inlet and integrated a passive bleed to minimize the size of separation bubbles. This study provided vital information for the development of scramjet units and CFD validation, demonstrating the efficacy of the bleed with a negligible mass flow penalty. Tam et al. [14] showed that bleeding low-momentum flows near the corners of a rectangular scramjet isolator improves performance by pushing shock systems downstream, with side-wall bleed slots proving more effective than center plane slots, guiding the experimental slot design for validation in wind tunnel tests at AFRL/PRA Test Cell 19. Kodera et al. [15] conducted experimental tests on a Mach 6 scramjet engine, and assessed boundary-layer bleeding and two-stage fuel injections to prevent unstart and enhance thrust. Results showed successful suppression of separation and thrust improvement, particularly with a full-strut configuration, while two-stage injections proved less effective due to combustion mode

limitations. Mitani et al. [16] illustrated that boundary-layer bleed systems effectively prevented engine unstart in Mach 4 and Mach 6 engines, extending the operating range while enhancing thrust, but two-stage fuel injections did not enhance thrust performance at Mach 6 due to insufficient mixing and combustion time. Herrmann et al. [17] conducted an experimental investigation of boundary-layer bleed configurations in a two-dimensional ramjet inlet, revealing their impact on inlet performance, shock-boundary layer interaction, and flow stability, and highlighting the challenges in optimizing pressure recovery, mass flow ratio, and stability point concurrently. Kouchi et al. [18] conducted numerical simulations of a scramjet engine with 0.65% boundary-layer bleeding and showed improved performance, suppressing separation and extending start limits. The experimental data were also consistent with the numerical results, emphasizing the usefulness of bleed in augmenting engine efficiency by preventing flow separation. Yue et al. [19] performed a similar study and noted how the injection of boundary layer bleed affects the thrust performance of scramjets, particularly attributing much of the effect to bleed mass flow rate. The study highlighted problems of maintaining thrust in the absence of bleed and simultaneously posed the need for better bleed systems to reduce these effects. Das and Prasad [20] performed numerical simulations on the effect of cowl deflection and back pressure on the performance of a mixed compression air intake, using FLUENT. It is concluded that in this case, a small amount of cowl deflection can be beneficial as it increases performance without the need to bleed. Das and Prasad [21] performed both numerical and experimental investigations in relation to unstart of intakes in ramjets for aerospace applications. In the course of this work, cowl deflection and boundary layer bleed have been investigated, and their outcomes demonstrated that cowl deflections were more effective than bleeds. This presented new opportunities to avoid separation in mixed compression intakes. Das and Prasad [22] demonstrated through experimental and computational investigations that introducing slight cowl deflection angles to a mixed compression air-intake designed for Mach 2.2 leads to improved performance and starting behavior, comparable to traditional bleeding methods. Reuben Vr and Rajamani [23] optimized a 2-D mixed-compression supersonic intake at Mach 2.4, finding that a 5-degree cowl deflection maximizes total pressure recovery, ensuring effective compression of the supersonic flow. Dalle et al. [24] investigated variable-geometry cowl designs for two-dimensional scramjet inlets, aiming to enhance performance across various Mach numbers. Gahlot and Singh [25] analyzed the starting behavior of a supersonic air intake using computational simulations with cowl porosity, revealing enhanced intake performance and flow quality. Merchant and Radhakrishnan [26] applied methods such as adjusting cowl deflection angles and bleed deflection angles to boost efficiency in a Mach 2.2 ramjet inlet. John and Senthilkumar [27] explored enhancing the performance of a supersonic air intake model with blunted leading edges, revealing improved mass capture and combustion stability alongside reduced shock wave boundary layer interaction and flow distortion, albeit with a slight decrease in total pressure recovery. Araújo et al. [28] presented an optimized two-dimensional mixed compression scramjet inlet design for spontaneous hydrogen combustion at supersonic speeds, demonstrating consistent thermodynamic properties and successful combustion chamber entry conditions

across various flight Mach numbers. Viswanath [29] stressed the persistent challenges in understanding turbulent interactions and Reynolds number effects in shock-wave-boundary-layer interactions, advocating for further research to address these complexities.

The current research status on scramjet engines indicates a significant gap in how incorporating bleeds of different dimensions and cowl deflections of different angles will affect the performance of the scramjet inlet. The current study is performed using different bleed dimensions and different cowl angle deflections separately, and then the focus is on how the integration of bleed and cowl angle will affect the performance of the scramjet inlet. The present analysis aims to bridge this gap by conducting a detailed computational analysis of Mach 5 scramjet inlets, with a particular focus on two-dimensional scramjet inlet-isolator geometry. Understanding how critical scramjets are to the advancement of aerospace engineering, this study seeks to improve the performance of scramjet engine inlets. Problems such as shoulder separation and intake system performance optimization were resolved using an active or passive flow control method as well as geometric alterations of scramjet inlets. The present study particularly investigates the influence of passive boundary layer bleed at the inlet throat on flow parameters with respect to 'long', 'removed' and 'short' types of bleed dimensions. The aim of this work is to obtain a broader understanding of the mechanisms that control scramjet inlet performance based on the fact that a previously studied 2-D inlet design has already produced some results. In the end, acquiring the knowledge to understand future advancements in hypersonic flight propulsion systems with the use of scramjet inlets is the ultimate aim. The focus of the work is narrowing the inlet flow to the expected discrimination level and increasing the total pressure recovery.

3 Methodology

The study now turns to the numerical implementation of ANSYS Fluent R18 aiming to study conditions at a Mach number of 5 and higher, which represents supersonic flow. The fluid is treated as an ideal gas with defined properties. The pressure and temperature applied to the free stream were 1228.5 Pa and 62.51 K respectively. Such conditions are essential in order to accurately represent the conditions of the high speed wind tunnel.

The equations solved in these simulations constitute a system of Reynolds-Averaged Navier–Stokes (RANS) equations, which consists of continuity equation, Navier–Stokes equations of motion and energy equation. For accurate representation of turbulence, this study utilizes the Shear Stress Transport (SST) k-ω model. This model is a two-equation model, which has been shown to be quite effective in predicting turbulence for a variety of flows, especially in high speed aerodynamics. The k-ω model consists of a complex mechanism wherein two transport equations are established: the first one is the turbulent kinetic energy (k) while the second one is the specific dissipation rate (ω). This model is best suited because it accounts for near wall treatment, which is important when considering aspects associated with high speed flows like supersonic flow.

A density-based solver is employed in the simulations, which is effective in solving compressible flows typical in high Mach numbers. Along with that, the solver also solves the conservation equation, which improves the stability and the convergence in the supersonic regimes. Also, the spatial discretization of the system is done using the

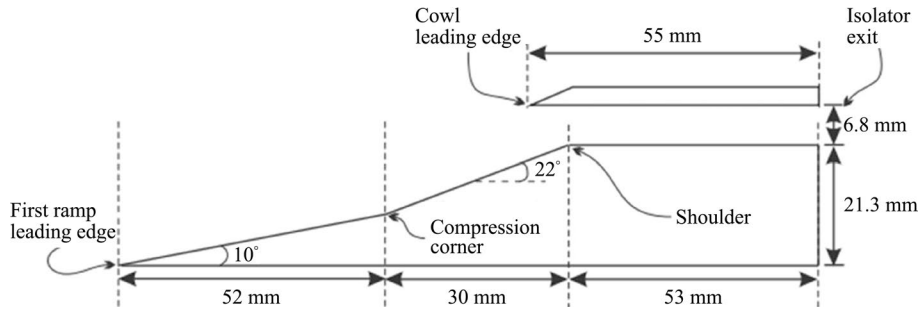

Fig. 2 Geometry of the scramjet inlet-isolator [1]

finite volume method, which is a mesh of control volumes. It is appropriate for complex shapes and even more difficult flow regimes.

Another fluid property, arguably the most significant, is the Viscosity, which is obtained through Sutherland's three coefficient method. The significance of this method is its ability to achieve temperature dependent viscosity calculations, which is vital for accurately modeling the flow of ideal gases. Sutherland's law links the dynamic viscosity to temperature factors, thus allowing one to realistically model the simulation at different temperatures and the corresponding fluid properties. Another important issue included in the sub-sequences is the appropriate grid independence test and solver validation performed to confirm that the adopted solver (ANSYS-Fluent) can be used for such numerical simulations.

3.1 Solver validation

The geometry of the inlet and the boundary conditions employed to validate the solver are explained in the sub-sections below, followed by the grid independence test.

3.1.1 Geometry

In order to validate the numerical solver, the inlet geometry from Che Idris et al. [1] has been adopted and is shown in Fig. 2. The figure consists of a 2D model of a scramjet inlet-isolator design that is used as base model for further simulations.

3.1.2 Typical mesh and boundary conditions

The far field is characterized by a Mach number of 5, with a freestream pressure of 1228.5 Pa and a temperature of 62.5 K, defining the overall boundary conditions for the system. For this study, we employed an unstructured mesh that incorporated a face mesh onto the inlet-isolator geometry for better accuracy compared to the rest of the domain. Inflation layers were implemented at the inside edges of the cowl and ramp to predict the variations of pressure, temperature, and Mach number in greater detail. This meshing technique ensured more detailed boundary layer regions, which captured all the intricate details necessary for the analysis. Face meshing combined with inflation layers enabled a detailed investigation of the scramjet inlet-isolator model. The computational domain, detailed mesh, boundary types employed in the case, and the near wall mesh are shown in Fig. 3.

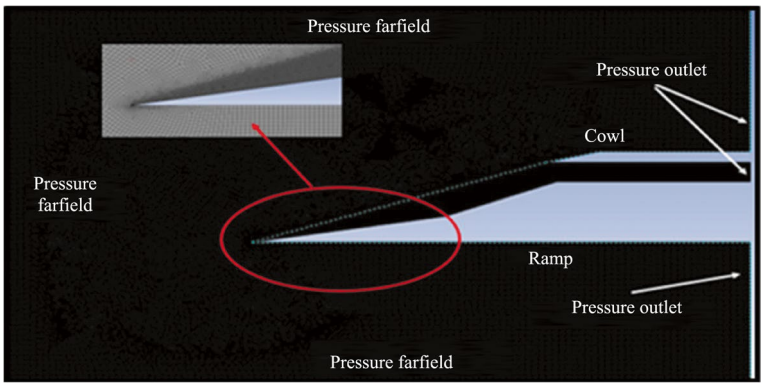

Fig. 3 Detailed mesh and boundary types

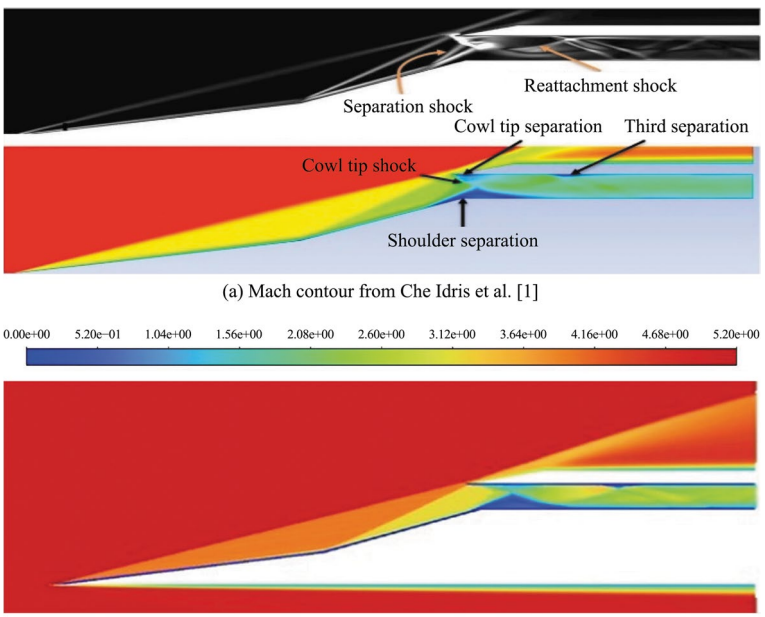

Fig. 4 Comparison of the Mach contours obtained from **a** Che Idris et al. [1] and **b** the validation case

3.1.3 Qualitative validation of Mach contour

Figure 4 shows a comparison of the Mach contour from Che Idris et al. [1] with that obtained from the current numerical simulations. A fair match of the flow features can be clearly observed.

3.1.4 Grid independence test

The grid independence test (GIT) was conducted using varying numbers of elements: coarse (0.15 million elements), medium (0.25 million elements), fine (0.35 million elements), and very fine (0.45 million elements). The configuration remained constant while simulations varied the number of mesh elements, as shown in Fig. 5. Results indicated that the fine mesh closely matches with the computational and experimental data, ensuring accuracy with a wall y^+ value below 1, facilitating a fair comparison with Che

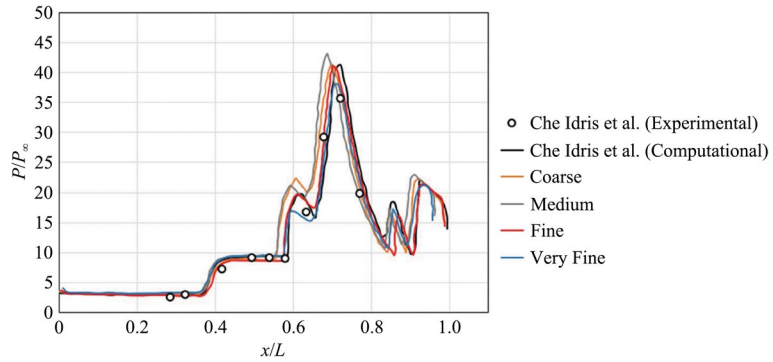

Fig. 5 GIT comparison graph of static pressure distribution on the ramp surface

Idris et al. [1], and validating the solver. Thus, the same mesh is adopted for further simulations in the present study.

4 Results and discussion

The present study explores methods to enhance inlet isolator performance, integrating a passive bleed mechanism and analyzing cowl deflection angles' effects. Furthermore, a combined approach is pursued, wherein the most promising configurations from both the bleed mechanism and the cowl deflection angle tests are integrated into a single geometry and the analysis on the same is studied. This integrated strategy aims to develop an optimized inlet design essential for enhancing engine performance and improving its pressure recovery.

4.1 Effect of bleed on the performance of scramjet inlet

The bleed dimensions used in this study follow the framework outlined by Häberle and Gülhan [9]. While the original inlet geometry by Che Idris et al. [1] lacked a bleed gap, the authors in the present study introduced four different bleed gap cases. In the present study, bleed gaps of 1.4045 mm, 2.809 mm, 4.2135 mm, and 5.618 mm were adopted by proportionally scaling from a prior work [9], which used bleed gaps of 5 mm, 10 mm, 15 mm, and 20 mm for a capture height of 100 mm. The corresponding capture height in this study is 28.09 mm. This approach maintains consistent aerodynamic behavior despite changes in dimensions, allowing accurate comparisons and valuable insights into optimizing aerodynamic surfaces and systems. The subsequent analysis examines the impact of these bleed gaps on inlet performance, as detailed in the following sections.

4.1.1 Bleed geometry

The bleed dimensions used in the present work are incorporated in the geometry with reference to Häberle and Gülhan [9]. The baseline geometry of the scramjet inlet incorporating passive bleed configurations with varying gap sizes is illustrated in Fig. 6.

The length $L1$ represents the bleed gap opening at the ramp, which determines the variation in pressure recovery at the isolator exit. In the further sub-sections, the effect of bleed gaps ($L1 = 1.4045$ mm, 2.809 mm, 4.2135 mm, 5.618 mm) on the inlet performance is presented. $L3$ (12.9 mm) corresponds to the bleed opening at the base. The

height $L2$ (28.09 mm) signifies the capture height of the inlet, and $L4$ (6.8 mm) denotes the outlet where compressed air exits the inlet and enters the combustor.

4.1.2 Effect of flow characteristics on Mach contours

In high-speed aerodynamic systems such as scramjet inlets, incorporating passive bleed mechanisms can significantly influence flow characteristics and overall performance. Passive bleed is primarily used to control and manage boundary layer behavior and shock interactions. By introducing bleed holes, high-pressure air can escape, which reduces the size and strength of separation bubbles induced by lip shocks on the ramp. Additionally, passive bleed mitigates the impact of strong shocks in the isolator section by relieving pressure, resulting in a smoother flow and reducing shock-induced separations. These improvements are typically visualized through Mach contours and pressure distribution plots, showing a more uniform flow and higher pressure recovery at the isolator exit.

Simulations without bleed, shown in Fig. 4b, often exhibit significant flow separations at critical points such as the shoulder, cowl tip, and isolator. These separations disrupt the flow, leading to lower pressure recovery and reduced efficiency of the scramjet inlet. In contrast, introducing bleed at the inlet isolator throat, as shown in Fig. 7a-d, demonstrates a marked improvement. The passive bleed reduces shoulder separation and influences the shock trains within the isolator, leading to a more controlled and stable flow.

Varying the dimension of the bleed gap allows for fine-tuning of the flow characteristics and pressure recovery. Smaller bleed gaps, such as 1.4045 mm, provide limited relief of pressure and boundary layer control, reducing separation bubbles but not fully mitigating the effect of shoulder separation at higher flow conditions. The intermediate bleed gap, like 2.809 mm, offers a balanced approach, providing sufficient pressure relief and better shock mitigation. This results in improved pressure recovery and more uniform flow through the isolator. Larger bleed gaps, such as 4.2135 mm and 5.618 mm, allow significant amounts of high-pressure air to escape, drastically reducing separation bubbles and mitigating shocks. However, excessively large gaps could lead to over-bleeding, potentially disrupting the desired flow dynamics and reducing the overall efficiency.

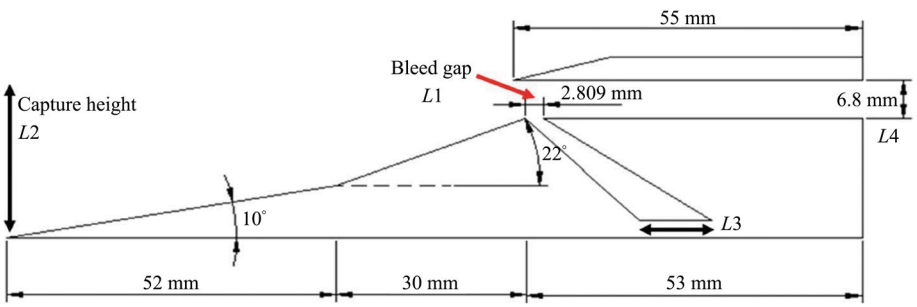

Fig. 6 Bleed $L1$ incorporated in four different cases with different dimensions of $L1 = 1.4045$ mm, 2.809 mm, 4.2135 mm, and 5.618 mm

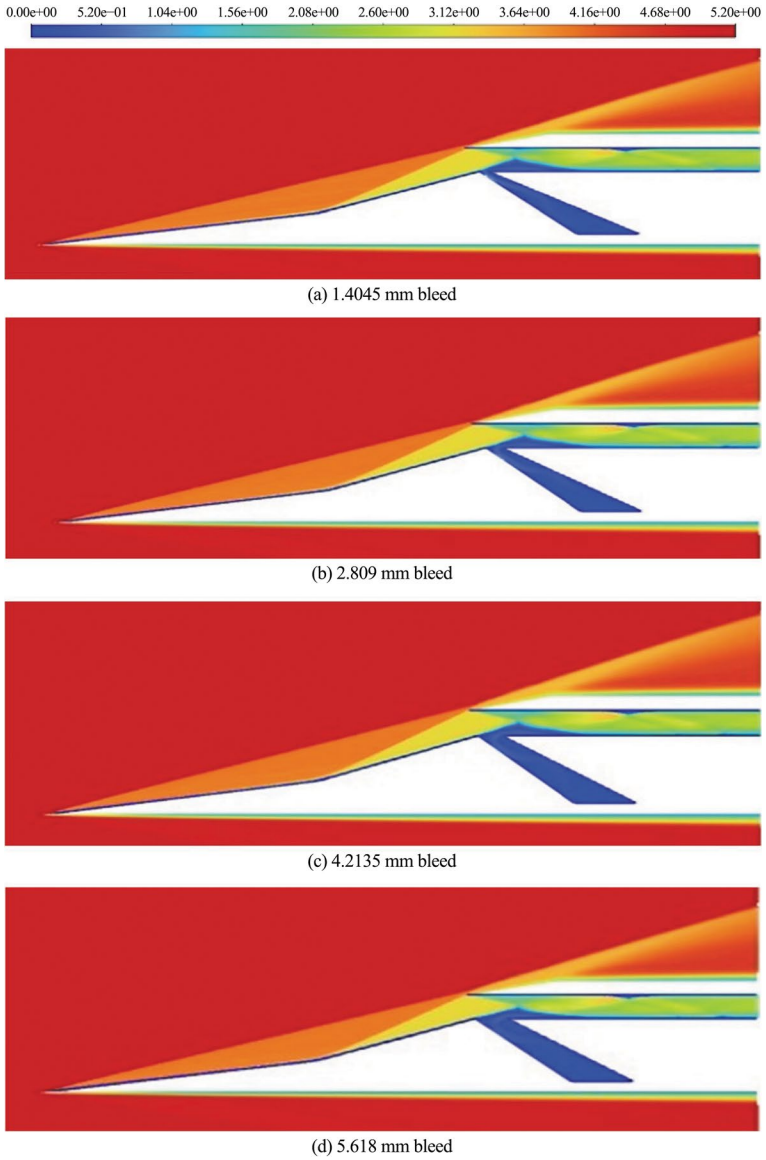

Fig. 7 Mach contours illustrating the impact of varying bleed dimensions on the flow within the scramjet inlet. **a** 1.4045 mm bleed, **b** 2.809 mm bleed, **c** 4.2135 mm bleed and **d** 5.618 mm bleed

4.1.3 Effect of bleed size on the surface pressure distribution on ramp

Compression within the scramjet inlet typically occurs through a discrete series of shock waves. Figure 8 represents the non-dimensionalized pressure distribution on ramp surface for various bleed dimensions, thereby depicting the Shock Boundary Layer Interactions inside the inlet-isolator body.

The pressure distribution data shown in Figure 8 highlight the influence of varying bleed gap sizes on the shock-boundary layer interaction and overall flow behavior at the inlet ramp surface. Each configuration, corresponding to a different bleed gap size (1.4045 mm, 2.809 mm, 4.2135 mm, and 5.618 mm), exhibits distinct characteristics in pressure recovery and separation control. Specifically, the segment from position 0 to 0.4 corresponds to the surface pressure distribution at the first ramp (10-degree ramp),

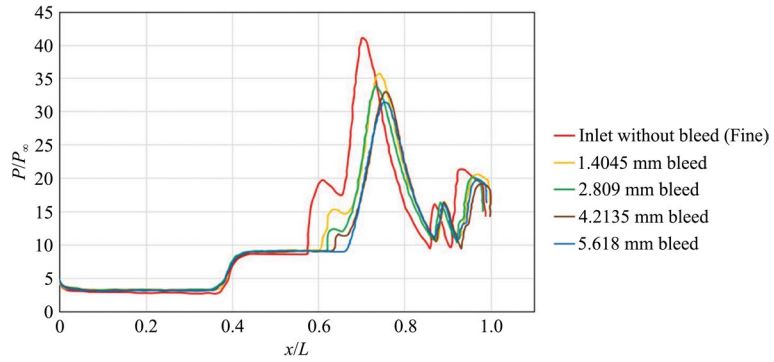

Fig. 8 Non-dimensionalized pressure distribution on ramp surface for various bleed dimensions

and the segment from 0.4 to 0.6 represents the surface pressure distribution at the second ramp (22-degree ramp). Beyond $x/L = 0.6$, there is a noticeable surge in pressure, indicative of the pressure distribution at the isolator section.

The analysis of bleed gap dimensions in scramjet inlets reveals a critical balance between shock mitigation and boundary layer control. A smaller bleed gap (1.4045 mm) provides only modest pressure relief, limiting its effectiveness in suppressing boundary layer separation, particularly under high dynamic pressure. In contrast, an intermediate gap (2.809 mm) offers the best trade-off, enhancing shock attenuation and pressure recovery while maintaining uniform isolator flow — key for high-speed efficiency. Larger gaps (4.2135 mm and 5.618 mm) improve separation control but risk over-bleeding, reducing total pressure recovery and disrupting optimal flow patterns. This underscores the need for precise bleed gap optimization to maximize scramjet inlet performance without compromising pressure stability.

Ultimately, the study highlights that bleed gap sizing must be carefully tailored to flight conditions, with intermediate gaps generally providing the best balance. Future designs could benefit from adaptive bleed systems or advanced CFD modeling to dynamically adjust airflow, ensuring peak efficiency across varying operational regimes. This optimization is essential for advancing hypersonic propulsion systems where even minor flow disruptions can significantly impact performance.

4.1.4 Effect of bleed size on the total pressure recovery at isolator exit

Figure 9 depicts a comparison of total pressure recovery for different bleed dimensions in free flow at the exit. This graph shows the total pressure recovery achieved at the outlet of the scramjet inlet. Total pressure recovery (π) is defined as the ratio between the stagnation pressure at the outlet of the inlet isolator and the initial stagnation pressure when the air enters the inlet. It serves as an indicator of the total pressure loss associated with the compression process.

In this study, we examine pressure recovery along the normalized length $L4$ (see Fig. 6) to evaluate how well the scramjet inlet maintains pressure — both with and without a bleed system. This measurement is crucial because it reveals how much energy is lost during compression, particularly due to the intense interplay between shock waves and the boundary layer.

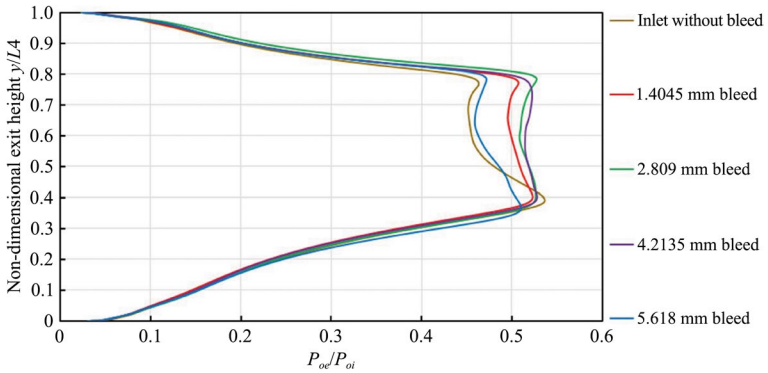

Fig. 9 Comparison of total pressure recovery for different bleed dimensions at the isolator exit

Table 1 Percentage increase in average total pressure recovery for various passive bleed configurations compared to the baseline (no-bleed) case

Case	Average total pressure recovery (π)	Percentage increase in average total pressure recovery
Validation case	0.287	NA
1.4045 mm bleed	0.296	3.316
2.809 mm bleed	0.346	20.697
4.2135 mm bleed	0.341	18.989
5.618 mm bleed	0.328	14.519

Why does this matter? Because higher pressure recovery means less wasted energy and better overall flow control — key factors in ensuring scramjet efficiency. Our findings highlight that optimizing bleed configurations can significantly improve performance by managing boundary layer growth and shock interactions.

To quantify these effects, we calculated average total pressure recovery values (shown in Table 1) using boundary layer data from both the upper and lower isolator surfaces. These results help us understand just how much bleed systems can reduce pressure losses and where further refinements might be needed.

4.2 Cowl deflection angle

The cowl deflection geometry adopted in the present study is as per the framework outlined by Das and Prasad [20]. The inlet geometry by Che Idris et al. [1] did not include a cowl deflection angle, and in the present study, the introducing of a total of five different cowl deflection angles of 1°, 2°, 3°, 4° and 5° has been studied respectively. The effect of cowl deflection angles on the inlet performance is then analyzed and reported in the further sub-sections.

4.2.1 Cowl deflection geometry

The cowl deflection angle used in the present work is incorporated in the geometry from Das and Prasad [20]. The scramjet inlet geometry used for analyzing the effects of cowl deflection angles is presented in Fig. 10.

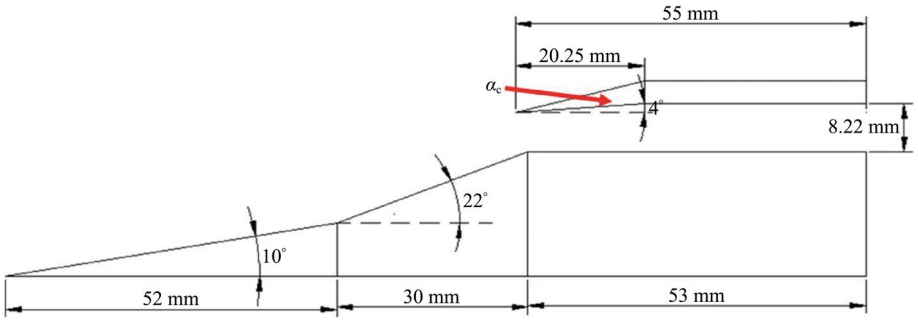

Fig. 10 Cowl deflection angle α_c incorporated in the present geometry with 5 different cases of $\alpha_c = 1°$, 2°, 3°, 4°, and 5°

The angle α_c represents the cowl deflection angle, which determines the variation in pressure recovery at the isolator exit. In the further sub-sections, the effect of various cowl deflections ($\alpha_c = 1°$, 2°, 3°, 4° and 5°) on the inlet performance is presented.

4.2.2 Effect of cowl deflection on Mach contours

The significance of Fig. 11a-e lies in its demonstration of how different cowl deflection angles influence the performance of scramjet inlets, with a specific focus on Mach contours. Introducing a cowl deflection angle in scramjet inlets is a critical strategy for addressing the challenges posed by shoulder separation. This deflection angle refers to the adjustment of the cowl, which is a movable component of the inlet, to alter the direction of incoming airflow. By positioning the cowl at an appropriate angle, several beneficial effects are realized.

To begin with, the boundary layer is able to reattach itself to the inlet surface due to the redirection of airflow. Shoulder separation occurs when the boundary layer becomes detached from the inlet surface, thus reducing efficiency of the airflow and increasing pressure losses. The introduction of a cowl deflection angle assists in redirecting the airflow in such a way that the boundary layer can reattach itself. This reattachment assists in keeping this boundary layer continuous and attached with a surface, thus reducing the separations extent and improving flow stability. In addition, the cowl deflection angle also controls the thickness of the boundary layer and the flow conditions inside the inlet. Moving the cowl allows engineers to manipulate the boundary layer for better aerodynamic performance and to lower all separation effects. This control works even better when trying to control how the flow behaves around sharp edges and corners, like the edge in the shoulder region of scramjet inlets. Finally, the cowl deflection angle helps with shock control, in so far as the inlet is concerned. Shoulder separation is usually found in regions where the shock wave close to the boundary layer folds and this creates a flow separation. The shock wave pattern might be shifted by adjusting the cowl deflection angle and therefore, the boundary layer will be less negatively affected. By keeping airflow smoother and lowering pressure losses, this serves to reduce the degree of separation and enhance overall inlet performance.

The trend that is noticed for the decrease in shoulder separation with the increase in cowl deflection angle matches with the variation in the flow physics of scramjet inlets. The experimental data at 1° of cowl deflection indicated an observable reduction in

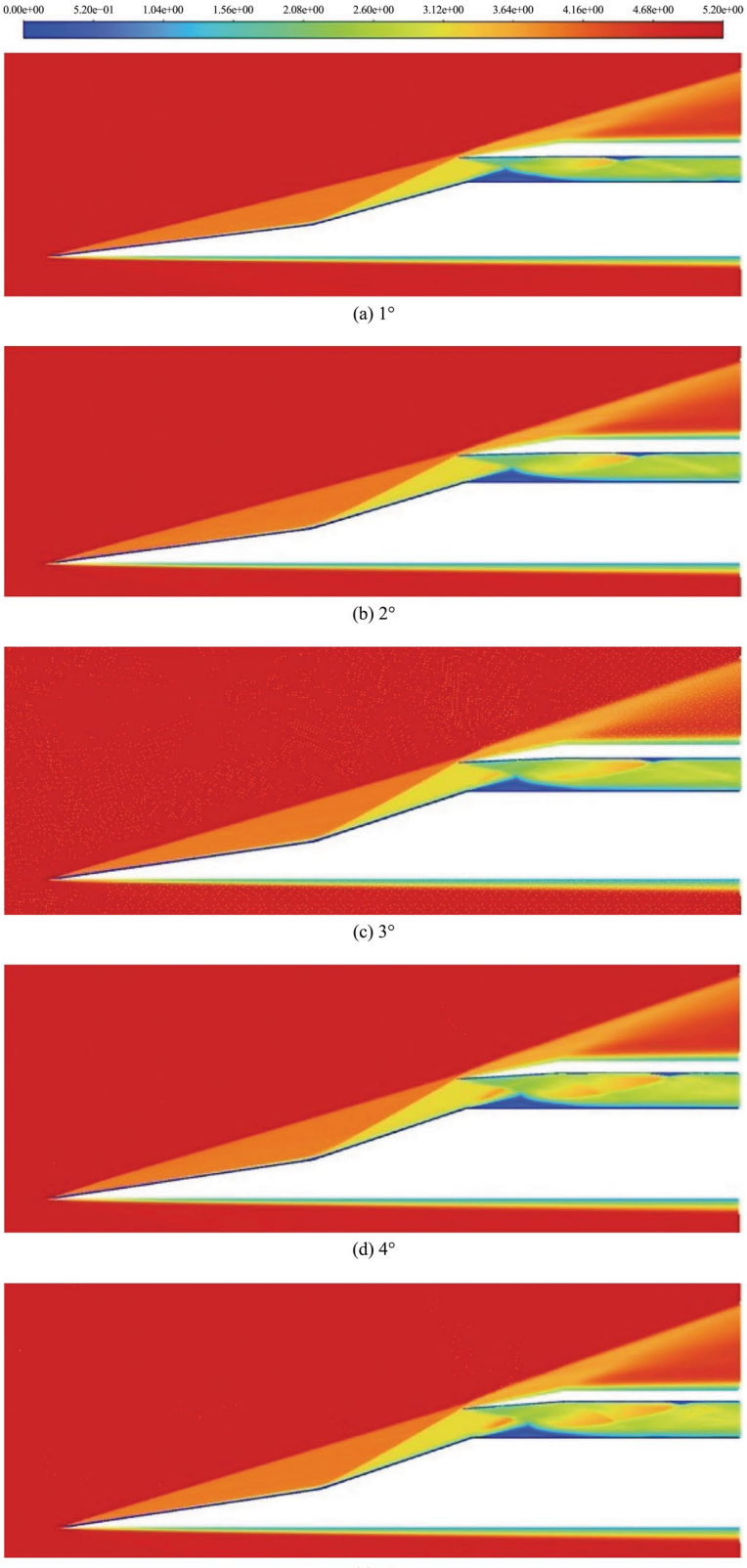

Fig. 11 Mach contours illustrating the impact of various cowl deflection angle configurations on the flow within the scramjet inlet isolator. **a** 1°, **b** 2°, **c** 3°, **d** 4° and **e** 5°

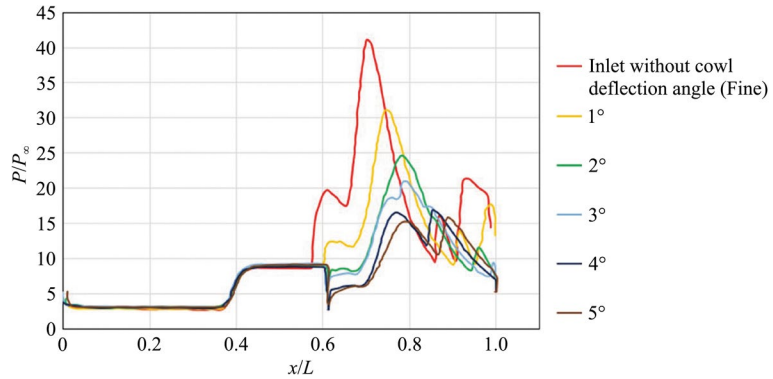

Fig. 12 Non-dimensionalized pressure distribution on ramp surface for various cowl deflection angle configurations

separation, and also showed that there is still considerable disruption to the airflow, with distinct separation visible, reducing the potential effectiveness of this variation. This indicates that the deflection angle of the cowl at this degree is not sufficient to properly control shock interactions and manage the boundary layer. With the cowl deflection angle extending to 2°, additional benefits are seen in terms of shoulder separation reduction. This suggests that the greater redirection of flow is aiding in improved boundary layer attachment to the inlet surface and reducing separation.

By increasing the cowl deflection angle up to 3°, a major enhancement in the flow physics was observed, with a considerable decrease in the shoulder separation. It indicates that the air flow is much more effective at this angle, thus causing less disturbances and allowing for better fluid flow patterns. For a cowl deflection angle of 4°, the best performance was observed in terms of minimizing flow separation. The flow physics suggests that this angle is also optimally suitable for governing the boundary layer thickness and shock circumstances, leading to a very effective inlet air flow. At a cowl deflection angle of 5°, a further reduction in flow separation was achieved; however, the extent of improvement is comparatively lower than that observed at 4°. This suggests that beyond a certain point, increasing the cowl deflection angle may lead to diminishing returns in terms of reducing shoulder separation, potentially due to over-adjustment of the airflow direction.

Lastly, it can be demonstrated that to a good extent, the shoulder separation problem is enhanced by including a cowl deflection angle in scramjet inlets. The angle of cowl deflection supports flow reattachment and increases pressure while managing boundary layer and shock interactions, which enhances and compliments inlet features, stability and pressure losses, and thus improves efficiency and effectiveness of scramjet propulsion systems.

4.2.3 Effect of cowl deflection angle on the surface pressure distribution on ramp

The compression in the scramjet inlet is usually done by a discrete number of shocks. Figure 12 represents the non-dimensionalized pressure distribution on ramp surface for various cowl deflection angle configurations, thereby depicting the Shock Boundary Layer Interactions inside the inlet-isolator body.

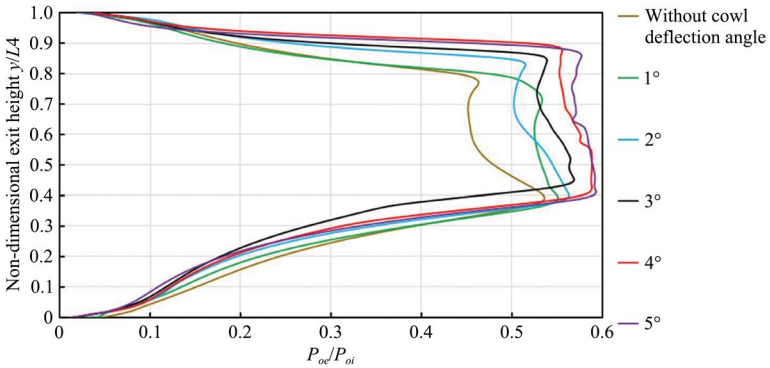

Fig. 13 Comparison of total pressure recovery for different cowl deflection angle configurations for free flow at the isolator exit

In Fig. 12, the pressure is plotted as a function of the non-dimensional length (x/L) to evaluate the effect of cowl deflection on inlet flow behavior. The pressure distribution along the ramp surface reveals the aerodynamic impact of varying cowl deflection angles on the scramjet inlet performance. As the deflection angle increases from 1° to 5°, a noticeable shift in the pressure peaks is observed, indicating changes in the location and intensity of shock interactions and boundary layer behavior. Specifically, the segment from position 0 to 0.4 corresponds to the surface pressure distribution at the first ramp (10-degree ramp), and the segment from 0.4 to 0.6 represents the surface pressure distribution at the second ramp (22-degree ramp). Beyond $x/L = 0.6$, there is a noticeable surge in pressure, indicative of the pressure distribution at the isolator section.

We can observe that there is a sudden increase in the surface pressure distribution at the isolator section, which leads to pressure loss. The diminished efficiency of the scramjet inlet can be attributed to three types of flow separation: shoulder separation, cowl tip separation, and the third separation occurring at the isolator.

The adoption of cowl deflection angles induces significant changes in the overall pressure distribution within scramjet inlets, highlighting the effect of varying cowl angles on inlet performance. Increasing the cowl deflection angle from 1° to 5° leads to noticeable alterations in pressure distribution. At 1°, there may be regions of higher pressure indicative of separation zones, while at higher angles like 4°, pressure distribution becomes more uniform with reduced separation. This trend underscores how adjusting cowl angles effectively redistributes pressure, optimizing airflow and minimizing flow disruptions within the inlet system. Our aim is to reduce the pressure loss and thus increase the pressure recovery on the inlet, which in turn improves the overall inlet performance, as discussed in the sections below.

4.2.4 Effect of different cowl deflection angles on the total pressure recovery at isolator exit

Figure 13 illustrates the comparison of total pressure recovery for various cowl deflection angle configurations in free flow at the isolator exit. This plot depicts the total pressure recovery achieved at the outlet of the scramjet isolator.

Table 2 presents the pressure recovery results for the validation case and the cases with cowl deflection angles.

Table 2 Comparison of average total pressure recovery for the baseline case (no cowl deflection) and various cowl deflection angles

Case	Average total pressure recovery (π)	Percentage increase in average total pressure recovery
Validation case	0.287	NA
1°	0.302	5.432%
2°	0.348	21.444%
3°	0.308	7.478%
4°	0.379	32.264%
5°	0.341	18.989%

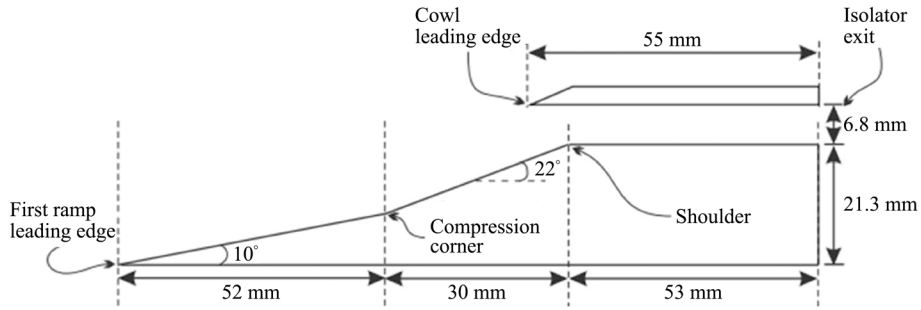

(a) Base case (without bleed and cowl deflection angle)

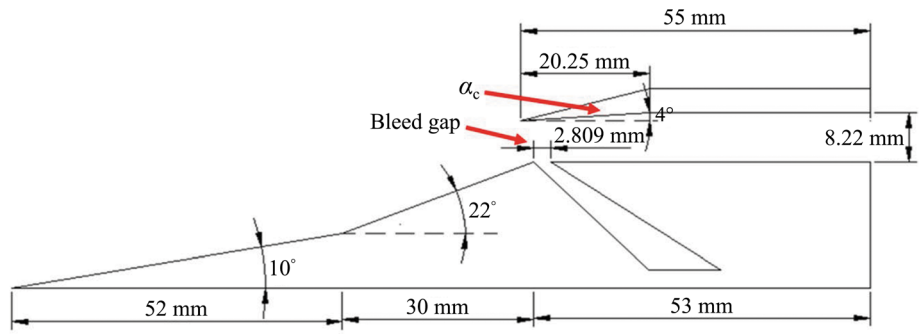

(b) Best cases of bleed ($L1$) and cowl deflection angle (α_c) geometry adopted from Fig. 6 and Fig. 10. $L1 = 2.809$ mm and $\alpha_c = 4°$

Fig. 14 Comparative analysis of the changes made in the geometry

4.3 Integrated bleed and cowl deflection angle configuration

Analysis in this section involves incorporating the optimal bleed case, with a bleed size of 2.809 mm, and the optimal cowl case, with a cowl deflection angle of 4°.

4.3.1 Integrated bleed and cowl deflection angle configuration geometry

The analysis presented in this subsection integrates the most effective bleed configuration, characterized by a bleed gap of 2.809 mm, with the optimal cowl deflection angle of 4°, as illustrated in Fig. 14. This combined configuration is specifically investigated to evaluate its impact on improving inlet flow characteristics, minimizing separation

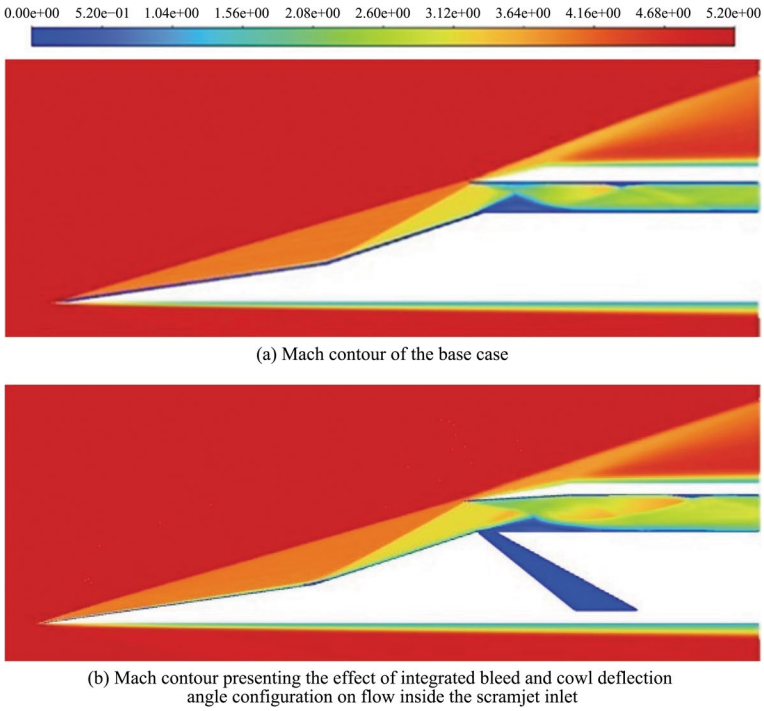

Fig. 15 Comparative study of the Mach contours. **a** Mach contour of the base case. **b** Mach contour presenting the effect of the integrated bleed and cowl deflection angle configuration on flow inside the scramjet inlet

regions, enhancing shock control, and ultimately maximizing pressure recovery and overall performance of the scramjet inlet.

4.3.2 Effect of integrated bleed and cowl deflection angle configuration on flow characteristics

The present study explores the influence of various cowl deflection angles on the performance of scramjet inlets, with a focus on Mach contours shown in Fig. 15. Findings demonstrate that when a certain cowl deflection is given, it significantly reduces lip-shock-induced separation on the inlet ramp and mitigates the effects of shock at the isolator section, resulting in improved pressure recovery at the isolator exit. This conclusion is reinforced by accompanying plots. Comparative analysis between cases with and without cowl deflection angles highlights distinct differences in flow separation patterns, including shoulder separation, cowl tip separation, and isolator separation. Incorporating a cowl deflection angle at the inlet throat diminishes the impact of shoulder separation, thereby influencing subsequent shock train behavior in the isolator section. Further investigation explores the influence of different cowl deflection angle configurations on pressure recovery at the isolator exit, offering valuable insights into optimizing inlet performance.

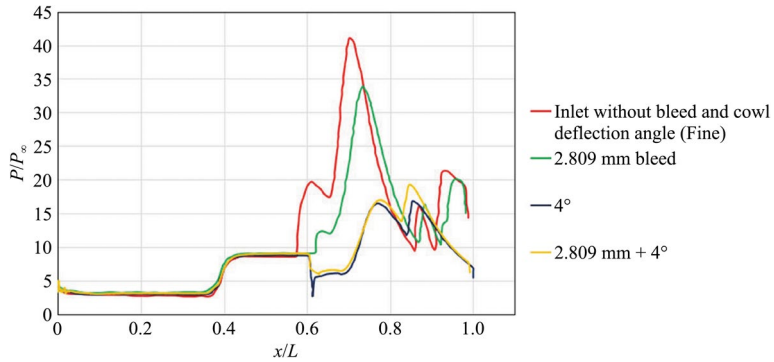

Fig. 16 Non-dimensionalized pressure distribution on ramp surface for the best cases with respect to the base case

4.3.3 Effect of integrated bleed and cowl deflection angle configuration on the surface pressure distribution on ramp

The compression in the scramjet inlet is usually done by a discrete number of shocks. Figure 16 represents the non-dimensionalized pressure distribution on ramp surface for various cowl deflection angle configurations, thereby depicting the Shock Boundary Layer Interactions inside the inlet-isolator body. In the integrated configuration, the bleed size and the cowl deflection angle are not entirely independent; their combined effect on the flow field can lead to nonlinear interactions. For example, a larger bleed size may mitigate some of the adverse effects caused by a large cowl deflection angle, such as boundary layer separation and shock-induced flow unsteadiness.

Figure 16 illustrates the surface pressure distribution along the normalized length (x/L) of the scramjet inlet under varying bleed gap sizes and cowl deflection angles. The analysis focuses on identifying how different geometric configurations influence pressure recovery, flow uniformity, and the suppression of separation zones within the inlet. Specifically, the segment from position 0 to 0.4 corresponds to the surface pressure distribution at the first ramp (10-degree ramp), and the segment from 0.4 to 0.6 represents the surface pressure distribution at the second ramp (22-degree ramp). Beyond $x/L = 0.6$, there is a noticeable surge in pressure, indicative of the pressure distribution at the isolator section. We can observe that there is a sudden increase in the surface pressure distribution at the isolator section, which leads to pressure loss.

4.3.4 Effect of integrated bleed and cowl deflection angle configuration on the total pressure recovery at isolator exit

Figure 17 compares total pressure recovery for the combined bleed and cowl deflection angle configuration at the scramjet inlet exit, serving as a measure of total pressure loss during compression.

The y-axis is represented by the length $L4$ (as referenced in Fig. 6), which is non-dimensionalized for this study, and the pressure recovery is measured at this location for the cases with bleed and without bleed. This metric is crucial for gauging the total pressure loss incurred during the compression process. The efficiency of total pressure, a key parameter, is notably impacted by interactions between shock waves and the boundary layer. Hence, pressure recovery emerges as a critical factor

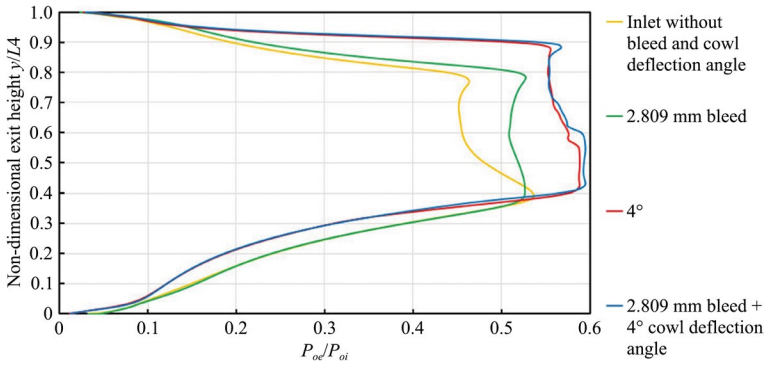

Fig. 17 Comparison of total pressure recovery for the best cases with respect to the base case

Table 3 Percentage increase in total pressure recovery for the best case of bleed and cowl deflection configurations compared to the validation case

Case	Total pressure recovery (π)	Percentage increase in total pressure recovery
Validation case	0.287	NA
2.809 mm bleed + 4° cowl deflection angle	0.382	33.335%

in assessing the pressure losses within the inlet-isolator system, contributing to the overall enhancement of the inlet's efficiency.

Table 3 are the pressure recovery results for the validation case and the cases with cowl deflection angles.

5 Conclusions

In summary, the assessment of the scramjet inlet-isolator performance revolved around total pressure efficiency (π), a critical metric capturing the loss of total pressure during compression. This loss can be attributed to various factors including shockwaves, boundary layer interactions, and viscous effects. The total pressure efficiency was calculated by comparing the stagnation pressure at the isolator exit with the freestream stagnation pressure at the inlet.

Introducing a 2.809 mm bleed led to a notable improvement in pressure recovery, enhancing efficiency by 20.697%. Similarly, employing a 4-degree cowl deflection angle resulted in a significant 32.264% increase in efficiency. These findings underscore the effectiveness of both the bleed mechanism and the cowl deflection angle in enhancing scramjet inlet performance.

However, when the 2.809 mm bleed and 4-degree cowl deflection angle are combined in the base geometry, the resulting efficiency improvement was relatively modest, at 33.335% compared to the base case. Surprisingly, upon comparing this combined configuration with the 4-degree cowl deflection angle alone, it was found that the former did not yield a significant efficiency enhancement. This observation suggests that, among the ten enhanced cases analyzed, the 4-degree cowl deflection angle emerged as the most effective in terms of enhancing total pressure efficiency.

Abbreviations

P	Static pressure (Pa)
P_∞	Freestream pressure (Pa)
P_{oi}	Total pressure at freestream (Pa)
P_{oe}	Total pressure at isolator exit (Pa)
L	Overall length of intake (mm)
$L1$	Bleed gap (mm)
$L2$	Capture height of intake (mm)
$L3$	Dimension of bleed at the base (mm)
$L4$	Isolator exit (mm)
π	Pressure recovery (-)

Acknowledgements
Not applicable.

Authors' contributions
All authors contributed equally to this work. All authors read and approved the final manuscript..

Funding
Not applicable.

Data availability
The datasets used and/or analyzed during the current study are available from the corresponding author on reasonable request.

Declarations

Competing interests
The authors declare that they have no competing interests.

Received: 9 June 2024 Revised: 19 November 2024 Accepted: 6 January 2025
Published online: 29 April 2025

References

1. Che Idris A, Saad MR, Zare-Behtash H et al (2014) Luminescent measurement systems for the investigation of a scramjet inlet-isolator. Sensors 14(4):6606–6632. https://doi.org/10.3390/s140406606
2. Im S, Do H (2018) Unstart phenomena induced by flow choking in scramjet inlet-isolators. Prog Aerosp Sci 97:1–21. https://doi.org/10.1016/j.paerosci.2017.12.001
3. Rodi PE, Emami S, Trexler CA (1996) Unsteady pressure behavior in a ramjet/scramjet inlet. J Propuls Power 12(3):486–493. https://doi.org/10.2514/3.24061
4. Smart MK (2010) Scramjet inlets (RTO-EN-AVT-185). NATO Research and Technology Organization, Neuilly-sur-Seine
5. Smart MK (1999) Optimization of two-dimensional scramjet inlets. J Aircr 36(2):430–433. https://doi.org/10.2514/2.2448
6. Ogawa H, Boyce RR (2012) Physical insight into scramjet inlet behavior via multi-objective design optimization. AIAA J 50(8):1773–1783. https://doi.org/10.2514/1.J051644
7. Suresh P, Manjunath S, Harshavardhana Gowda MR et al (2020) Study of flow optimization in mixed compression inlet with cowl deflection. Int Res J Eng Technol 7(5):1531–1536
8. Neale MC, Lamb PS (1965) Tests with a variable ramp intake having combined external/internal compression, and a design Mach number of 2.2 (CP No 805). Aeronautical Research Council, London
9. Häberle J, Gülhan A (2008) Experimental investigation of a two-dimensional and a three-dimensional scramjet inlet at Mach 7. J Propuls Power 24(5):1023–1034. https://doi.org/10.2514/1.33546
10. Häberle J, Gülhan A (2007) Internal flowfield investigation of a hypersonic inlet at Mach 6 with bleed. J Propuls Power 23(5):1007–1017. https://doi.org/10.2514/1.29669
11. Häberle J, Gülhan A (2007) Investigation of the flow field of a 2D SCRAM-jet inlet at Mach 7 with optional boundary layer bleed. In: 43rd AIAA/ASME/SAE/ASEE joint propulsion conference & exhibit, Cincinnati, 8-11 July 2007. https://doi.org/10.2514/6.2007-5068
12. Häberle J, Gülhan A (2006) Investigation of the performance of a scramjet inlet at Mach 6 with boundary layer bleed. In: 14th AIAA/AHI space planes and hypersonic systems and technologies conference, Canberra, 6-9 November 2006. https://doi.org/10.2514/6.2006-8139
13. Häberle J, Gülhan A (2008) Investigation of two-dimensional scramjet inlet flowfield at Mach 7. J Propuls Power 24(3):446–459. https://doi.org/10.2514/1.33545
14. Tam CJ, Eklund D, Behdadnia R et al (2005) Investigation of boundary layer bleed for improving scramjet isolator performance. In: AIAA/CIRA 13th international space planes and hypersonics systems and technologies conference, Capua, 16-20 May 2005. https://doi.org/10.2514/6.2005-3286
15. Kodera M, Tomioka S, Kanda T et al (2003) Mach 6 test of a scramjet engine with boundary-layer bleeding and two-staged fuel injection. In: 12th AIAA international space planes and hypersonic systems and technologies, Norfolk, 15-19 December 2003. https://doi.org/10.2514/6.2003-7049
16. Mitani T, Sakuranaka N, Tomioka S et al (2005) Boundary-layer control in Mach 4 and Mach 6 scramjet engines. J Propuls Power 21(4):636–641. https://doi.org/10.2514/1.7978

17. Herrmann D, Blem S, Gülhan A (2011) Experimental study of boundary-layer bleed impact on ramjet inlet performance. J Propuls Power 27(6):1186–1195. https://doi.org/10.2514/1.B34223
18. Kouchi T, Mitani T, Masuya G (2005) Numerical simulations in scramjet combustion with boundarylayer bleeding. J Propuls Power 21(4):642–649. https://doi.org/10.2514/1.7967
19. Yue L, Xu X, Chang X (2013) Theoretical analysis of effects of boundary layer bleed on scramjet thrust. Sci China Phys Mech Astron 56:1952–1961. https://doi.org/10.1007/s11433-013-5257-4
20. Das S, Prasad JK (2009) Cowl deflection angle in a supersonic air intake. Defence Sci J 59(2):99–105
21. Das S, Prasad JK (2008) Alleviation of unstart of a supersonic intake adopting cowl deflection and bleed. In: 12th Asian congress of fluid mechanics, Daejeon, 18-21 August 2008
22. Das S, Prasad JK (2010) Starting characteristics of a rectangular supersonic air-intake with cowl deflection. Aeronaut J 114(1153):177–189. https://doi.org/10.1017/S0001924000003626
23. Reuben Vr L, Rajamani A (2022) Study on performance of ramjet intake by changing the cowl angle. IOP Conf Ser Mater Sci Eng 1258:012042. https://iopscience.iop.org/article/10.1088/1757-899X/1258/1/012042
24. Dalle DJ, Torrez SM, Driscoll JF (2011) Performance analysis of variable-geometry scramjet inlets using a low-order model. In: 47th AIAA/ASME/SAE/ASEE joint propulsion conference & exhibit, 31 July - 03 August 2011. https://doi.org/10.2514/6.2011-5756
25. Gahlot NK, Singh NK (2019) Starting characteristic of supersonic mixed compression air intake with cowl porosity. J Phys Conf Ser 1240:012008. https://doi.org/10.1088/1742-6596/1240/1/012008
26. Merchant V, Radhakrishnan J (2017) Design and optimization of supersonic intake. IOP Conf Ser Mater Sci Eng 225:012298. https://doi.org/10.1088/1757-899X/225/1/012298
27. John B, Senthilkumar P (2018) Alterations of cowl lip for the improvement of supersonic-intake performance. J Appl Fluid Mech 11(1):31–41. https://doi.org/10.29252/jafm.11.01.28164
28. Araújo PPB, Pereira MVS, Marinho GS et al (2021) Optimization of scramjet inlet based on temperature and Mach number of supersonic combustion. Aerosp Sci Technol 116:106864. https://doi.org/10.1016/j.ast.2021.106864
29. Viswanath PR (1988) Shock-wave-turbulent-boundary-layer interaction and its control: A survey of recent developments. Sadhana 12:45–104. https://doi.org/10.1007/BF02745660